Lenka JAKUBOVIČOVÁ[1], Milan SÁGA[2], Milan VAŠKO[3]

# NUMERICAL STUDY OF INFLUENCE OF MUTUAL SLEWIG OF ROLLER BEARING RINGS ON THE PRINCIPAL STRESSES AT CONTACT AREA

**Summary.** Article deals with influence of mutual slewing of roller bearing rings on the principal stresses and their distribution at the contact area. Profile of rolling element is logarithmic. Roller bearing has been loaded by maximum specified load only in radial direction according to the ISO/TS 16281. In practice, the real roller bearings are not loaded only in the radial direction. Therefore, the angle $\alpha$ has been gradually slewed from $\alpha = 0'$ to $8'$ and equivalent principal stresses have been evaluated. This change influenced on contact conditions and contact stress distribution has changed.

**Keywords:** roller bearing, Contact analysis, Hertz theory, Static load-carrying capacity, Finite element method, ADINA system.

# ANALIZA NUMERYCZNA WPŁYWU PRZENIESIONEJ ZMIANY KĄTA NACHYLENIA NA GŁÓWNE NAPRĘŻENIA W REJONIE STYKU

**Streszczenie.** Artykuł jest poświęcony wpływom nachylenia pierścieni łożyska walcowego na wielkość i rozłożenie trzech głównych naprężeń na płaszczyźnie styku. Profil łożyska tocznego (walca) jest logarytmiczny. Łożysko walcowe zostało obciążone maksymalnym dopuszczalnym obciążeniem statycznym wyłącznie w kierunku promienia, zgodnie z normą ISO/TS 16281. W praktyce realne łożyska walcowe nie są obciążane wyłącznie w kierunku promienia, dlatego też kąt nachylenia pierścieni łożyska walcowego $\alpha$ stopniowo zmieniał się od $\alpha = 0'$ do $8'$, a odpowiednie główne naprężenia były oceniane dla poszczególnych położeń. Zmiana ta miała wpływ na warunki styku oraz na zmianę rozłożenia naprężeń podczas styku.

**Słowa kluczowe:** łożysko walcowe, analiza kontaktowa, teoria Hertza, podstawowa wytrzymałość statyczna łożyska, metoda elementów skończonych, system ADINA.

## 1. INTRODUCTION

The early theory of contact mechanics was developed by Russian scientists at the beginning of the 20th century with the main emphasis on mathematical methods

[1] Faculty of Mechanical Engineering, University of Žilina, Žilina, Slovakia, e-mail: lenka.jakubovicova@fstroj.uniza.sk
[2] Faculty of Mechanical Engineering, University of Žilina, Žilina, Slovakia, e-mail: milan.saga@fstroj.uniza.sk
[3] Faculty of Mechanical Engineering, University of Žilina, Žilina, Slovakia, e-mail: milan.vasko@fstroj.uniza.sk

in analytical solutions contact form. In engineering analyzes, simplified results have been used for long time. Classic examples include Hertzian pressure (Hertz, 1882), Carter's rolling theory (Carter, 1926) and Winkler elastic foundations (Winkler, 1867) are known to many mechanical and building engineers [6, 7, 8].

For design of the standard parts and its components are set standard procedures in ISO standards. However, non-standard methods of loading and dynamic contact problems require more detailed and advanced solutions. Based on the experience an international technical standard has been established (Technical specification: Rolling bearing – Methods for calculating the modified reference rating life for universally loaded bearings) [1]. The static load-carrying capacity is taken as the load acting on a bearing such that in the most heavily loaded area of contact the total residual strain developed in the rolling elements and races does not exceed 0.0001 of the diameter of the rolling element [1]. The deformation arises from an equivalent load which is equal to the calculated bearing rating.

The radial static load rating for all cylindrical roller bearings (roller, needle, spherical, tapered) is 4000 MPa which correspond to computational contact stresses at the center of the most loaded contact area of rolling element with the raceway.

The basic static radial load rating for roller bearings is

$$C_{or} = 44\left(1 - \frac{D_{we} \cdot \cos\alpha}{D_{pw}}\right) i\, Z\, L_{we}\, D_{we} \cdot \cos\alpha\,, \tag{1}$$

where $D_{we}$ – roller diameter applicable in the calculation of load rating, $D_{pw}$ – pitch diameter of roller elements, $Z$ – number of rolling elements, $L_{we}$ – effective roller length.

The main focus of this article is to analyze roller bearings stresses by finite element method [1]. The outer and inner ring of cylindrical roller bearing will be slewed against each about the specified angle $\alpha$ = 0', 2', 4', 6', 8', fig. 1.

Safety coefficient $f_s$ represents a measure of safety against too large plastic deformations at the rolling elements contact points. If the bearings have easy and especially silent rotation, they require high value of safety coefficient

$$f_s = \frac{C_{or}}{P_{or}}\,, \tag{2}$$

$f_s$ = 2.5 to 4 – for extremely high requirements, $f_s$ = 1.2 to 2.5 – for high requirements,
$f_s$ = 0.8 to 1.2 – for normal requirements, $f_s$ = 0.5 to 0.8 – for low requirements.

$P_{or}$ is the static equivalent radial force [N]. Especially high safety factor is required for structures that have higher requirements for safety (bearings used in wind turbines, lifts gearboxes, wheels for railway carriages, etc.). A set of calculations in the gradual slewing of the roller bearing rings with safety of $f_s$ = 4, the roller bearing load represents only 0.25 times the basic static rating of the bearing, i.e. load rate $f_F$ = 0.25.

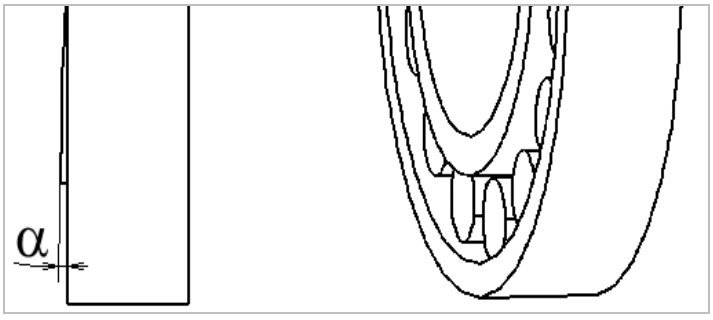


Fig. 1. Mutual slewing of the roller bearing rings together with rolling elements
Rys. 1. Wzajemne nachylenie pierścieni łożyska walcowego wraz z elementami tocznymi

## 2. CALCULATION OF LOGARITHMIC ROLLER PROFILE AND BASIC STATIC RADIAL RATING

If a purely cylindrical roller is loaded, edge stresses will occur, which can substantially exceed the calculated Hertzian pressure [4]. Therefore rollers are usually profiled, they are produced to the roller bearing with logarithmic profile or "KB" profiles.

In our case, the profile of roller bearing element is logarithmic [2]. For rollers having a length $L_{we} \le 2.5D_{we}$ a stepwise defined profile function

$$P(x_k) = 0.00035\, D_{we} \cdot \ln\left[\frac{1}{1-(2\,x_k / L_{we})}\right], \tag{3}$$

where $x_k$ is x-coordinate from the center of roller. Basic dimensions of bearing are shown in table 1.

Table 1

Basic dimensions of analyzed roller bearing

| | |
|---|---|
| Outer diameter | $D$ = 180 mm |
| Bearing bore diameter | $d$ = 100 mm |
| Width of inner and outer ring | $B$ = 34 mm |
| Outer diameter of the inner ring | $F_w$ = 120 mm |
| Diameter of rolling element | $D_{we}$ = 21.5 mm |
| Pitch diameter of rolling elements | $D_{pw}$ = 141.5 mm |
| Effective roller length | $L_{we}$ = 25 mm |
| Number of rolling elements | $Z$ = 16 |

By substituting values from the table 1 into (1) is obtained the value of the basic static radial load rating for roller bearing, $C_{or}$ = 300 848 N. Finite element calculations were made for the rate of load $f_F$ = 1, therefore the applied loading radial force from (2) is $P_{or}$ = 300 848 N.

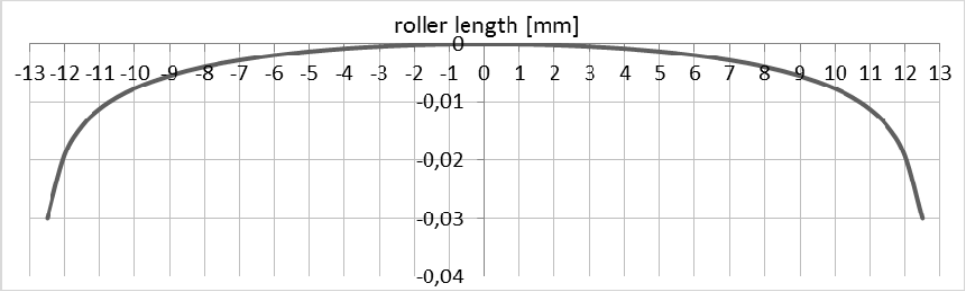


Fig. 2. Logarithmic profile of rolling element, rolling element diameter is scaling factor 1:200
Rys. 2. Profil logarytmiczny elementu tocznego, w kierunku średnicy walca to stosunek 1:200

## 3. PREPARATION OF A MODEL FOR FE ANALYSIS

FE software ADINA was used for FE analysis. One quarter of the roller bearing model was created for the purposes of the analysis. In the model, the profile of roller bearing element is logarithmic [1], fig. 2. Eight-node quadratic elements were used to create finite element mesh for the FE model. Mesh size of the model was 2 mm. The higher mesh density was used in the inner and outer rings contact point of rolling elements.

At least 6 elements on contact ellipse width were used. According to Hertz theory [3], the width of the contact ellipse is $b = 0.74 \cdot 10^{-3}$ m [2]. The isotropic linear elastic material was used ($E = 2.1 \cdot 10^5$ MPa, $\mu = 0.3$) [4, 5]. The shaft was replaced by constrains. Non-linear contact problem was solved by Full-Newton iteration method.

## 4. STRESS-STRAIN FE ANALYSIS

Stress state is evaluated in the most loaded element of the roller bearing. Stresses $\sigma_1$, $\sigma_2$ and $\sigma_3$ are evaluated at gradual slewing of the roller bearing rings, $\alpha$ = 0' to 8' with step size $\Delta\alpha$ = 2'. The whole model and roller detail is showed on figure 3. We can see stress $\sigma_3$ at the angle $\alpha$= 0' and at the load rate $f_F$ = 1.

Cylindrical roller bearings are machine components, for which reliability and durability and also static and dynamic bearing capacity are evaluated on base of acquired values of stresses. In this case the values of principal stresses $\sigma_1$, $\sigma_2$, $\sigma_3$ were used for evaluation of stress in contact. Nodes on edge were selected like is shown on figure 4.

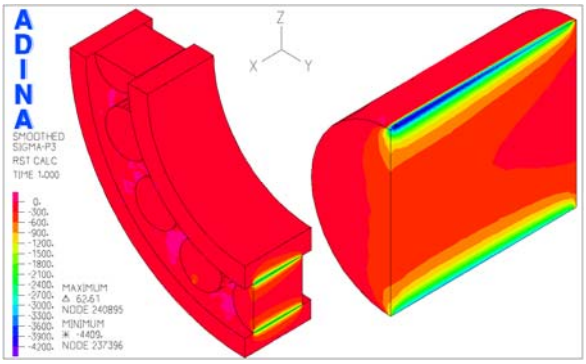


Fig. 3. Stress $\sigma_3$ at load rate $f_F$ = 1, angle $\alpha$ = 8'
Rys. 3. Naprężenie $\sigma_3$ przy stopniu obciążenia $f_F$ = 1, kąt $\alpha$ = 8'

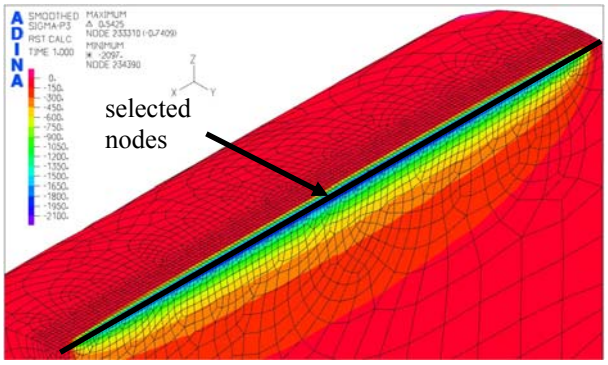


Fig. 4. Selected nodes on the edge of cylindrical roller, stress $\sigma_3$ at angle $\alpha$ = 0', load rate $f_F$ = 0.25
Rys. 4. Punkty węzłowe leżące na skraju walca, na-prężenie $\sigma_3$, kąt $\alpha$ = 0', stopień obcią-żenia $f_F$ = 0,25

For processing of the results, graphical depiction of fields of monitored values for defined slewing angles of bearing rings and for individual load rates was required. Courses of these none smoothed principal stresses $\sigma_1$, $\sigma_2$ and $\sigma_3$ are presented on figures 5 to 7 and maximal values of stress were obtained. Table 2 shows a gradual increase of the $\sigma_1$, $\sigma_2$ and $\sigma_3$ stresses values at gradual load rate $f_F$ = 0.25 to 1.0 (gradual safety $f_s$ = 4.0 to 1 steps by $\Delta f_s$ = 0.5).

Table 2

Percentage of principal stress increased at slewing angle $\alpha$=8' , load rate $f_F$ = 0.25 to 1

| load rate $f_F$ (safety $f_s$) | stress $\sigma_1$ [MPa] – [%] | stress $\sigma_2$ [MPa] – [%] | stress $\sigma_3$ [MPa] – [%] |
|---|---|---|---|
| 0.25 (4.0) | -1255 (+17.5 %) | -1908 (+29.2 %) | -2537 (+20.7 %) |
| 0.285 (3.5) | -1328 (+16.9 %) | -2095 (+32.2 %) | -2692 (+20.4 %) |
| 0.333 (3.0) | -1375 (+12.1 %) | -2306 (+32.5 %) | -2876 (+19.7 %) |
| 0.4 (2.5) | -1519 (+13.8 %) | -2463 (+23.8 %) | -3037 (+16.5 %) |
| 0.5 (2.0) | -1688 (+10.8 %) | -2751 (+17.1 %) | -3327 (+14.1 %) |
| 0.666 (1.5) | -1886 (+7.6 %) | -3088 (+12.4 %) | -3684 (+10.7 %) |
| 1 (1.0) | -2249 (+6.6 %) | -3720 (+10.9 %) | -4409 (+11.0 %) |

The gradual change and increase the value of the principal stress $\sigma_3$ on the roller surface depends else on the angle$\alpha$. Table 3 shows a gradual increase in the value of the $\sigma_1$, $\sigma_2$ and $\sigma_3$ stresses at gradual slewing angle $\alpha$ = 0' to 8' of roller bearing rings. The increase in the

maximum value of stress is quadratic. Maximum value of stress $\sigma_3$ at the angle $\alpha$ = 0' is $\sigma_3$ = -3972 MPa and at the angle $\alpha$ = 8' is $\sigma_3$ = -4409 MPa. The stress value $\sigma_3$ increased by 11.0%.

Table 3

Maximum value of stresses at gradual slewing of roller bearing rings $\alpha$=0' to 8', $f_F$ = 1

| angle $\alpha$ | stress $\sigma_1$ [MPa] – [%] | stress $\sigma_2$ [MPa] – [%] | stress $\sigma_3$ [MPa] – [%] |
|---|---|---|---|
| 0' | -2110 (0 %) | -3354 (0 %) | -3972 (+0 %) |
| 2' | -2111 (+0.5 %) | -3396 (+1.25 %) | -3978 (+0.15 %) |
| 4' | -2164 (+2.55 %) | -3492 (+4.1 %) | -4141 (+4.25 %) |
| 6' | -2228 (+5.6 %) | -3619 (+7.9 %) | -4280 (+7.85 %) |
| 8' | -2249 (+6.6 %) | -3720 (+10.9 %) | -4409 (+11.0 %) |

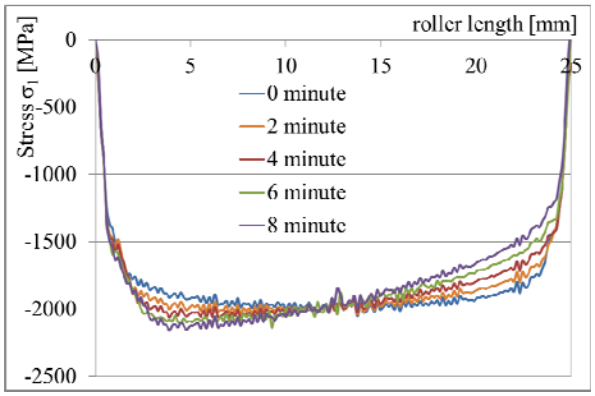


Fig. 5. Stress $\sigma_1$ at angle $\alpha$=0' to 8', load rate $f_F$=1
Rys. 5. Naprężenie $\sigma_1$ dla kąta $\alpha$=0' ÷ 8', $f_F$=1

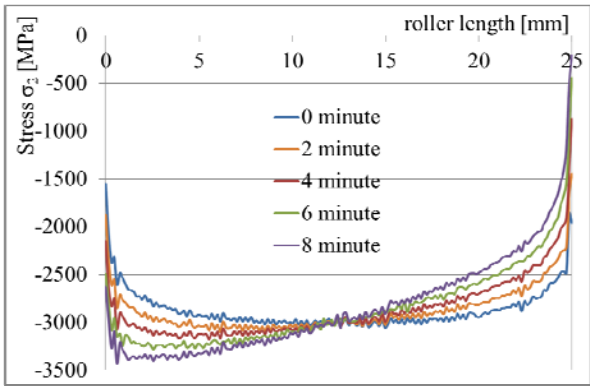


Fig. 6. Stress $\sigma_2$ at angle $\alpha$=0' to 8', load rate $f_F$=1
Rys. 6. Naprężenie $\sigma_2$ dla kąta $\alpha$=0‘ ÷ 8‘, $f_F$=1

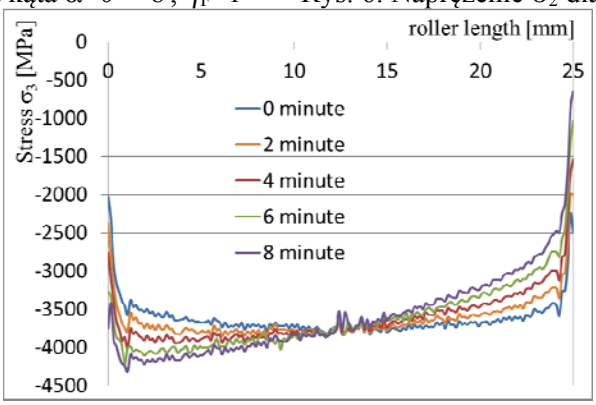


Fig. 7. Stress $\sigma_3$ at angle $\alpha$ = 0’ to 8’, load rate $f_F$ = 1
Rys. 7. Naprężenie $\sigma_3$ dla kąta $\alpha$=0' ÷ 8', stopień obciążenia $f_F$=1

We can observe gradual movement of maximal values of individual principal stress components from the center of the roller in the direction of ring slew. Gradual rise of stresses occurs. The largest increase of the third principal stress $\sigma_3$ occurred at load level $f_F$ = 0.25 by 20.7% and second principal stress $\sigma_2$ by 29.2%.

Based on that consideration, it is possible to establish, that the contact pressure at the load rate $f_F$ = 0.25 increases about quarter of its permitted value. It means that the safety coefficient $f_s$ is not equal to $f_s$ = 4, but it is equal to safety coefficient $f_s$ = 2.5. It is not sufficient and the system failure can occur.

In the next part were analyzed maximal stresses at contact surface. Magnitude and course of the third principal stress $\sigma_3$ at the contact surface of the roller at mutual slewing of rings by angle $\alpha = 0'$ and load rate $f_F = 1$ is plotted on the figure 8. Values of stress $\sigma_3$ are interpolated.

Contours for interpolated values of the third principal stress $\sigma_3$ referring to figure 8 are plotted on figure 9.

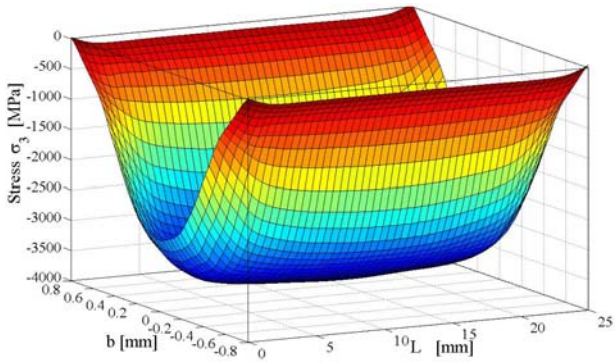


Fig. 8. Stress $\sigma_3$ at angle $\alpha = 0'$, load rate $f_F = 1$

Rys. 8. Naprężenie $\sigma_3$ dla kąta $\alpha = 0'$, stopień obciążenia $f_F = 1$

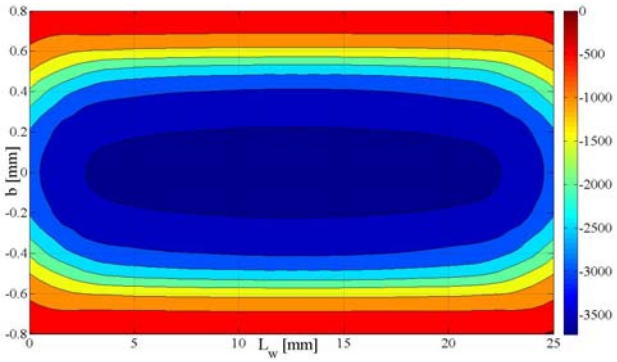


Fig. 9. Contour of stress $\sigma_3$ at angle $\alpha = 0'$, load rate $f_F = 1$

Rys. 9. Obwiednia naprężenia $\sigma_3$ dla kąta $\alpha = 0'$, stopień obciążenia $f_F = 1$

The last position of gradual slewing of rings of roller bearing is slewing by angle $\alpha = 8'$. The value of the third principal stress at the contact surface for that angle and load rate is depicted below on figure 10 for interpolated values.

Contours referring to third principal stress $\sigma_3$ for the angle of slewing $\alpha = 8'$ are depicted on figure 11 for interpolated values.

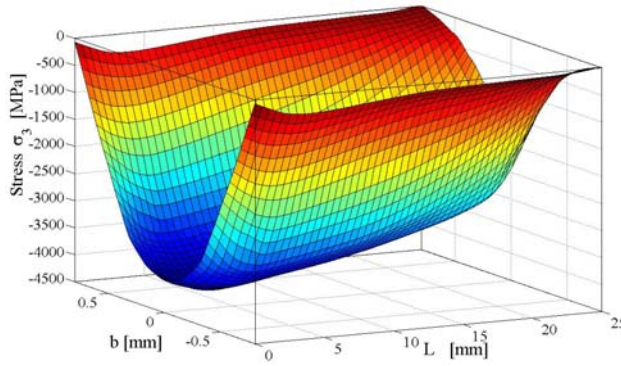


Fig. 10. Stress $\sigma_3$ at angle $\alpha = 8'$, load rate $f_F = 1$

Rys. 10. Naprężenie $\sigma_3$ dla kąta $\alpha = 8'$, stopień obciążenia $f_F = 1$

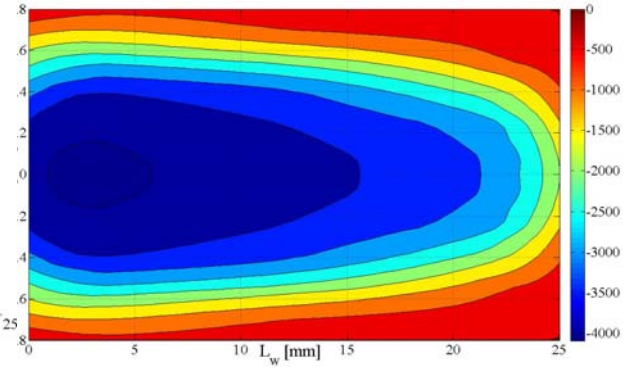


Fig. 11. Contour of stress $\sigma_3$ at angle $\alpha = 8'$, load rate $f_F = 1$

Rys. 11. Obwiednia naprężenia $\sigma_3$ dla kąta $\alpha = 8'$, stopień obciążenia $f_F = 1$

If we have a roller bearing with similar dimensions loaded by 1.0 $C_{or}$ (for example), the increase of compressive stress $\sigma_3$ can be estimated for a specific angle by this quadratic polynomial function. The relation is a function of three variables:

- slewing angle of cylindrical roller bearing rings $\alpha = 0', 2', 4', 6', 8'$,
- loading rate of cylindrical roller bearing $f_F = 0{,}25 \div 1$,
- the maximal value of the third principal stress $\sigma_3$.

In the same way were interpolated other two main stresses $\sigma_1$ $\sigma_2$. The degree of polynomial was gradually changed in the direction of ring slewing and load rate. For every approximation was evaluated the coefficient of correlation of used function approximation.

In the direction of slewing angle were values approximated by polynomial of third degree and in the direction of load rate by polynomial of second degree. This degree of polynomial can be considered adequately accurate. The surfaces are described by the equation 4.

$$\sigma_i = \mathbf{T}_i \cdot \mathbf{P}\,, \tag{4}$$

where $i = 1, 2, 3$,

$$\mathbf{T}_1 = \begin{bmatrix} -523.2 \\ -4.578 \\ -2372 \\ -8.047 \\ 34.58 \\ 787.3 \\ 0.071 \\ -0.3623 \\ -19.52 \end{bmatrix}^{\mathrm{T}}, \mathbf{T}_2 = \begin{bmatrix} -385.9 \\ -23.31 \\ -4729 \\ -9.77 \\ 54.74 \\ 1765 \\ 0.3229 \\ 3.062 \\ -43.8 \end{bmatrix}^{\mathrm{T}}, \mathbf{T}_3 = \begin{bmatrix} -1146 \\ 31.95 \\ -4177 \\ -27.37 \\ 24.35 \\ 1341 \\ 1.851 \\ 3.11 \\ -30.43 \end{bmatrix}^{\mathrm{T}} \text{ and } \mathbf{P} = \begin{bmatrix} 1 \\ \alpha \\ f_F \\ \alpha^2 \\ \alpha \cdot f_F \\ f_F^2 \\ \alpha^3 \\ \alpha^2 \cdot f_F \\ \alpha \cdot f_F^2 \end{bmatrix}. \tag{5}$$

In our case the value of radial static load for cylindrical roller bearing stated by technical standard ISO 76 equals to 4000 MPa what corresponds with computational contact stresses in the centre of the most loaded zone of contact between rolling element and raceway.

On the figure 12 is depicted the dependency of the first principal stress $\sigma_1$ for load rate $f_F = 0.25$ to 1.0 and for slewing angle of bearing rings $\alpha = 0'$ to $8'$. Maximum stresses $\sigma_1$, $\sigma_2$ and $\sigma_3$ at load rate $f_F = 0.25$ to 1 and at mutual slewing of roller bearing rings angle $\alpha = 8'$ are shown in figures 12 to 14.

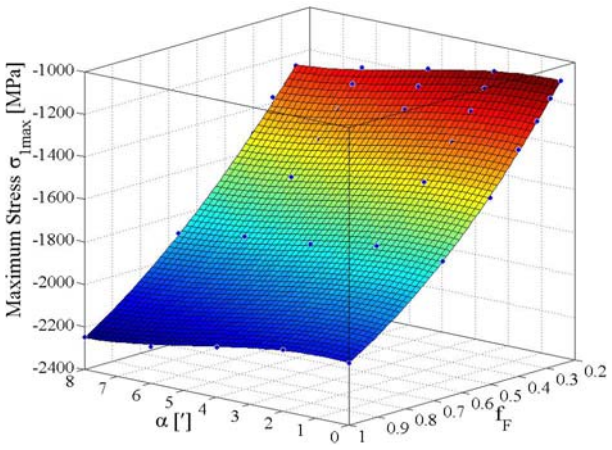


Fig. 12. Maximum stress $\sigma_1$ at angle $\alpha = 0'$ to $8'$, load rate $f_F = 0.25 \div 1$

Rys. 12. Maksymalne naprężenie $\sigma_1$ dla kąta $\alpha = 0' \div 8'$, stopień obciążenia $f_F = 0{,}25 \div 1$

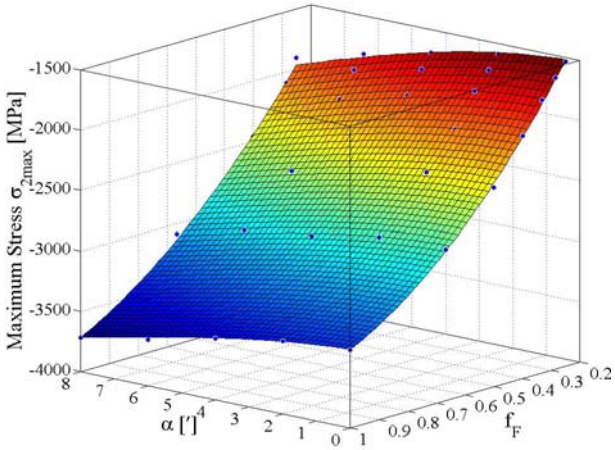


Fig. 13. Maximum stress $\sigma_2$ at angle $\alpha = 0'$ to $8'$, load rate $f_F = 0.25 \div 1$

Rys. 13. Maksymalne naprężenie $\sigma_2$ dla kąta $\alpha = 0' \div 8'$, stopień obciążenia $f_F = 0{,}25 \div 1$

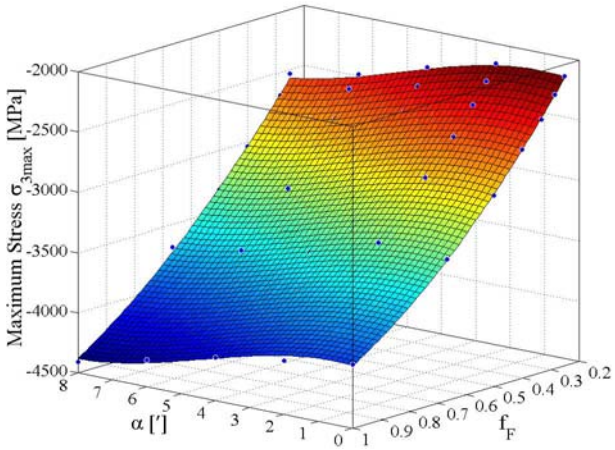


Fig. 14. Maximum stress $\sigma_3$ at angle $\alpha$ = 0' to 8', load rate $f_F$ = 0.25 ÷ 1
Rys. 14. Maksymalne naprężenie $\sigma_3$ dla kąta $\alpha$ = 0' ÷ 8', stopień obciążenia $f_F$ = 0,25 ÷ 1

## 5. CONCLUSION

The main goal of this article was the influence study of mutual slewing of roller bearing rings and load rate on principal stresses in contact area. The finite-element program ADINA was used for the analysis of this problem.

The set of calculations in the gradual slewing of the roller bearing rings was made with the various values of safety coefficient $f_s$. The influence of two parameters was expressed by polynomials of high degree (second and third). Stress $\sigma_3$ decreases about 11%, it means from -3972 MPa to -4409 MPa. It can be the reason of the limit state generation.


## Acknowledgement

*Development of optimum technology for the analysis of limit states of structural elements in contact, ITMS code 26220220118.*

Európska únia
Európsky fond regionálneho rozvoja

Agentúra Ministerstva školstva, vedy, výskumu a športu SR pre štrukturálne fondy EÚ

Operačný program VÝSKUM a VÝVOJ

The project is co-financed by the European Union.


## Bibliography


1. Technical specification ISO/TS 16281. Rolling bearings – Methods for calculating the modified reference rating life for universally loaded bearings, 2008.
2. http://www. tribology-abc.com/calculators/e2_3.htm
3. Hills D.A., Nowell D., Sackfield A.: Mechanics of Elastic Contacts. Butterworth & Heinemann, Oxford 1993.
4. Leitner B., Kopas P.: The vector autoregressive moving average models asa tool for stochastically loaded dynamic systems identification. Machine Dynamics Research, No. 4, Vol. 34, 2010, p. 32-41.

5. Melicher R., Handrik M.: Analysis of Shape Parameters of Tool for ECAP Technology. Acta Mechanica Slovaca, Vol. 12, No. 3-C, 2008, p. 273-284.
6. Žmindák M., Riecky D.: Meshless Modelling of Laminate Mindlin Plates under Dynamic Loads. Communications, Vol. 14, No. 3, 2012, p. 24-31.
7. Sapietová A., Dekýš V.: A design and Optimization of the Fully Automatic Shunting Mechanism, Advances in Mechanisms Design, Mechanisms and Machine Science 8, Vol. 10, 2012, p. 421-427.
8. Lack T., Gerlici J.: Modified Strip Method utilization for wheel/rail contact stress evaluation, 9th international conference on contact mechanics and wear of rail/wheel systems (CM2012), 27-30 August 2012, Chengdu, China: proceedings. Chengdu: Southwest Jiaotong University, 2012, p. 87-89.
9. Kaššay P., Homišin J.: Determining the Properties of Pneumatic Flexible Shaft Couplings with Wedge Flexible Elements 2013. Zeszyty Naukowe Politechniki Śląskiej, s. Transport, Vol. 81, No. 1896, p. 59-67.
10. Krajňák J., Grega R.: Comparison of three different gases and their influence on dynamic properties one-bellow and two-bellows flexible pneumatic coupling, 2013. Zeszyty naukowe Politechniki Śląskiej, s. Transport, No. 81, p. 79-84.
11. Grega R., Krajňák J.: The application of pneumatic flexible coupling in conveyor drive-2013. Technológ. Roč. 5, č. 4, s. 51-54.
12. Kaššay P., Homišin J., Grega, R., Krajňák J.: Comparation of selected pneumatic flexible shaft couplings, 2011. Zeszyty Naukowe Politechniki Śląskiej, Vol. 73, No. 1861, p. 41-48.